FE simulation and experimental tests of high-strength structural bolts under tension

Published in:
Journal of Constructional Steel Research

Document Version:
Peer reviewed version

Queen's University Belfast - Research Portal:
Link to publication record in Queen's University Belfast Research Portal

FE Simulation and Experimental Tests of High Strength Structural Bolts under Tension

Ying Hu*, Le Shen, Shidong Nie, Bo Yang

School of Civil and Structural Engineering, Chongqing University, P.R. China, Postcode: 400045

Key Laboratory of New Technology for Construction of Cities in Mountain Area (Chongqing University), Ministry of Education, Chongqing, P.R. China, Postcode: 400045

Wei Sha*
School of Natural and Built Environment, Queens University of Belfast, Belfast BT7 1NN, UK

* y.hu@cqu.edu.cn (Y. Hu); w.sha@qub.ac.uk (W. Sha)

Highlights

- Bolts mating with nuts of higher class can lead to a higher probability in failure
- 8.8 structural bolts mating with bright nuts failed by thread stripping
- In the numerical simulation, influence of different material laws was small
- Some discrepancy in load-displacement relationship can be observed
- Numerical simulation was capable of representing the failure mechanisms

FE Simulation and Experimental Tests of High Strength Structural Bolts under Tension

ABSTRACT

Experimental tests has been completed for high strength 8.8 bolts for studying their mechanical performance subjected to tensile loading. As observed from these tests, failure of structural bolts has been identified as in one of two ways: threads stripping and necking of the threaded portion of the bolt shank, which is possibly due to the degree of fit between internal and external threads. Following the experimental work, a numerical approach has been developed for demonstration of the tensile performance with proper consideration of tolerance class between bolts and nuts. It has been found that the degree of fit between internal and external threads has been identified as a critical factor affecting failure mechanisms of high strength structural bolts in tension, which is caused by the machining process. In addition, different constitutive material laws have been taken into account in the numerical simulation, demonstrating the entire failure mechanism for structural bolts with different tolerance classes in their threads. It is also observed that the bolt capacities are closely associated with their failure mechanisms.

Keywords: structural bolt; numerical simulation; tolerance class; high temperature

1 Introduction

In modern steel construction, bolted connections are commonly used for joining steel beams and columns of a steel-framed building, transmitting the loads from one steel member to another. Based on their stiffness, strength and rotation capacity, a classification system of flexible, semi-rigid and rigid connections has been proposed by Nethercot et al. [1] and Goto and Miyashita [2]. In these systems, the ductility of a connection (rotation capacity) has been used as a reference for its classification. The rotation capacity of a bolted connection depends on the deformation capacity of its components and the interaction between the individual components making up the connection [3]. During fire, structural performance of bolted steel connections may be unpredictable due to deterioration of material properties of the steel components, i.e. tensile strength and Young's modulus, affecting their interaction with each other.

Bolted connections are vulnerable to two failure mechanisms during fire or in a non-fire situation: thread stripping and necking of the threaded portion of the bolt shank [4, 5]. Thread stripping causes the reduction or loss of tensile resistance of structural bolts, which has been demonstrated in the experimental tests of Kirby [6] and Hu et al. [7]. They also indicated that the performance of assembled bolts and nuts at high temperatures would be affected by factors related to the manufacturing process and the variation in tolerance classes. In general, the manufacturing process of 8.8 structural bolts may comprise several main stages: pickling, straightening, forging, threading, quenching and tempering, and finally coating. Manufacturing nuts normally involves hot forging operation, where steel rods are cut into small pieces and heated up to 1200 ℃. Then these pieces are punched into small hexagons and drilled to threads cutting. The threading operation may involve thread rolling or thread cutting, and the degree of fit between threads is determined by their tolerance class.

More than twenty metals and alloys may be employed for coating the threads of bolts and nuts to varying thicknesses, with the most common coating processes being zinc plating, galvanizing, Xylan coating and black oxidation (blackening). Laurilliard [8] points out that all coatings affect the performance of a bolted connection, physically and chemically. There are two basic issues associated with the performance of bolts affected by the coating method, hydrogen embrittlement and diametral over-tap (or thread over-tapping). Hydrogen embrittlement is a delayed brittle failure mechanism during static loading at stress levels well below the tensile strength of the material due to the presence of hydrogen absorbed and retained in the base metal during the coating process [8]. Major factors affecting the degree of hydrogen embrittlement in high-strength bolts and nuts have been summarized in the reference [8].

Most 8.8 high-strength bolts and nuts have a plated zinc layer or a black appearance due to the coating process, which is capable of depositing a thin adherent metallic or non-metallic layer. In order to accommodate extra coatings, internal threads are commonly over-tapped by about 0.35-0.53 mm as bolt threads are never made undersized [9-11].

In 1995, Kirby from British Steel developed an experimental program on grade 8.8 high-strength structural bolts in fire, studying their fire performance under shear and tension [6]. The most valuable finding in this research is a strength reduction model

produced for structural bolts at high temperatures. Reference [6] also reported the failure mechanisms observed of structural bolts with different types of Property Class eight nuts. Hanus et al. [12] investigated the behavior of Grade 8.8 bolts under natural fire conditions (considering the influence of heating-cooling cycles), and found that the mechanical behavior was seriously affected by temperature variation during the heating and cooling phases. Lou et al. [13] completed an extensive series of fire tests on structural bolts (grades 8.8 and 10.9) to look into the after-fire performance. Different cooling conditions (cooling in air and cooling in furnace) were taken into account in Lou et al.'s research to produce the feasible reduction factors for bolts after fire. However, in the preceding research efforts, there are two substantial issues associated with bolt performance: the coating process and the constitutive relationship of the component material, that are not fully studied.

This paper begins with a brief review of the experimental research work completed on 8.8 high-strength structural bolts, with a discussion of their tolerance classes and component strengths. In reference to different specifications, a numerical model has been developed with consideration of influence of the coating operation and different material laws, investigating the failure mechanisms of high strength structural bolts with different coatings using a numerical approach. This paper also presents results of finite element simulations conducted to examine the various modeling techniques, and comments on the numerical results are provided finally.

2 Experimental program

In the published specifications, structural bolts may be ordered in accordance with British Standard (BS 4190), European Standard (BS EN ISO 4014), DIN Standard (DIN 976), or American Standard (ASTM 490); most of their provisions are consistent with ISO Standard (ISO 898). The launched experimental program for 8.8 high-strength structural bolts (to BS 4190 and BS EN ISO 4014) was intended to verify an approach (proposed by Kirby) that 8.8 high-strength bolts assembled with nuts of one property class higher are capable of preventing the premature failure at high temperatures [6]. The component tests have been carried out at the Structural Laboratory of the University of Sheffield. Looking into their failure mechanisms using the numerical approach is another objective after this experimental program. Experimental details are stated in the followed sections.

2.1 Test Specimens

The high-strength Grade 8.8 bolts are made from low carbon steels or alloy steels in accordance with BS 4190:2001 and BS EN ISO 4014:2001, followed by a quench and temper heat treatment to develop the required mechanical properties. They normally have proof stress $\geq$ 640 N/mm^2 and tensile strength 800~981 N/mm^2, corresponding nearly to ASTM A490 and ISO 898. To fully discover the influence of helical threads, an experimental program was developed for structural bolts. They are ordered to BS 4190 (British Standard) and BS EN ISO 4014 (European Standard). It should be noted that different tolerance classes are stipulated for threads in these two standards. The European standard has a more stringent control in bolt and nut threads. In this program, structural bolts were partially-threaded and 100 mm long; structural nuts were prepared with two types, bright finish and black finish, for two different

strength levels (Grade 8 and Grade 10, respectively). Accessible details of bolts and nuts are displayed in Table 1 for this experimental program.

Table 1: Accessible information for ordered bolts and nuts

Bolt Set	Tensile and yield strength (N/mm^2)	Nut proof load stress (N/mm^2)	Bolt Specification	Nut Specification	Tolerance Class
Bolt Group A	800	1000	BS 4190, Br*	BS 4190, Ba*	7H/8g
Bolt Group B	800	1000	BS EN ISO4014, Ba*	BS EN ISO4032, Ba*	6H/6g
Bolt Group C	800	800	BS 4190, Br*	BS 4190, Br*	7H/8g
Bolt Group D	800	800	BS EN ISO4014, Ba*	BS EN ISO4032, Br*	6H/6g

Br* = Bright finish (zinc plated), Ba* = Black finish (black oxide coating)

However, it should be noted that structural bolts or nuts ordered may have two types of coating conditions, zinc plating and black oxidation. As already known, coating of structural components is utilized for intention of creating an anti-corrosive layer to prevent oxidation and corrosion of these products under atmospheric conditions. There are more than 20 metals and alloys in use for coating of these components, but with varying coating thicknesses and coating processes. For examples, zinc plating and black oxide are the most commonly used approaches for deposit of the coating layer to threads. Black oxide is a low cost conversion coating where oxidizing salts are used to react with the iron in steel alloys to form magnetite (Fe_3O_4). This reaction produces a microscopic oxidation layer without affecting the dimensional aspects of internal and external threads (adding less than 5 to 10 millionths of an inch to the dimension of the surface), developing an attractive and durable anti-corrosion protection for these steel components. For better corrosion resistance steel fasteners can be electroplated for producing a shiny silver finish, with a sacrificial thickness layer in the component surface. As documented in the reference of Laurilliard [8], fastener coatings may affect the behavior of these components in a bolted connection physically and chemically. There are two identified issues closely associated with the behavior of high-strength bolts with zinc-plated coatings: hydrogen embrittlement and diametral over-tapping. However, the hydrogen embrittlement will not be further discussed in this context, and more care will be given to the phenomenon of threads stripping possibly due to diametral oversize tapping.

In study of the premature failure of internal threads, we should recall the knowledge of tolerance classes in the literature [14]. Tolerance class describes the looseness or tightness (the degree of fit) of internal and external threads, represented as a figure and letter combination, the digital number indicating the tolerance and the letter standing for the fundamental deviation (or tolerance position), as shown in Table 2. Thus, the minimum total clearance between corresponding dimensions of threads (including external and internal) is the sum of their fundamental deviations. The maximum total clearance is obtained by adding the thread tolerances to the minimum total clearance. However, it should also be noted that oversize tapping of nuts and internal threads to tolerance class 6AZ or 6AX is required for zinc coated fasteners in accordance with ISO 10684 [15]and ISO 965-5 [10], when the mating bolts or screws or external threads are manufactured to tolerance position g or h in accordance with the specifications below.

Table 2: Fundamental deviations and tolerances

Specification	Class of fit	Tolerance class					
		External thread (mm)			Internal thread (mm)		
		Tolerance	Fund. deviation		Tolerance	Fund. deviation	
BS 4190	Free	8	g	0.042	7	H	0.000
BS 3692	Medium	6	g	0.042	6	H	0.000
BS EN ISO 4014/4032	Medium	6	g	0.042	6	H	0.000
ISO 10684/965-5	Free	-	g	0.042	6	AZ	0.350
			h	0.000	6	AX	0.530

In the previous discussion, it is very clear that both internal and external threads may have tolerance classes applied to their basic profiles. However, the actual profiles of internal and external threads must never cross or transgress these basic (theoretical) profiles, which has already been taken as an essential principle in design of threads. As revealed in Table 2, for threads with zinc coating, the oversize tapping created a fundamental deviation to make internal threads slightly larger to be capable of depositing a thin and adherent metallic layer on the material surface of bolts and nuts. For this purpose, internal threads may be reduced by 0.35 to 0.53 mm in their basic profiles in accordance with ISO 965-5 and ISO10684. In the accepted experience, the coating layer space gathered may be determined as eight times the coating layer thickness, and internal threads are commonly over-tapped by 0.4 mm. For example, if assuming that the coating layer thickness is 48 microns (this value is an average of the collected zinc coating thicknesses, mechanical plating requiring 55 microns, zinc spraying 48 microns and hot-dip galvanizing 43 microns), the coating space required is about 0.38 mm (eight times of the coating layer thickness), which is just fitted into the minimum clearance between internal and external threads, as the provisions in the above mentioned standards. However, the zinc coating layer may further weaken threads of nuts mechanically or chemically, which might lead to higher possibility in premature thread stripping failure of bolt assemblies, which is an essential reason for us to look into it.

2.2 Test device and test procedure

For testing of 8.8 high-strength bolts, a high temperature testing chamber was built to accommodate a compression-and-tension testing machine, and thermo-couple wires were attached to the specimen, as shown in Fig.1. The tension tests were carried out under displacement control with a strain rate of 0.001-0.003 /min for both elastic and plastic regions, recommended by Kirby [6]. Each specimen was heated up to a target temperature, maintained for 15 minutes for stabilization to establish a uniform temperature distribution. A slow heating rate of 2.5 ℃/min was adopted for all fire tests, which exerted a small influence on the ultimate load-carrying capacities due to a prolonged "soaking" period [6].

For material properties, tension tests were carried out in accordance with BS 3688-1 on round specimens machined from 8.8 high strength structural bolts. The dimensions of the specimens used for these tests are in accordance with EN 10002-5 and ISO 6892-1. The gauge length was 25 mm. An INSTRON 8862 high-precision actuator system was used for tensile coupon tests, and calibration was completed before testing. The tension test was performed at a strain rate of 0.001/min to provide

proof strength values up to 5%, beyond which the strain rate was raised to 0.025/min and maintained until fracture. Three specimens were tested at room temperature.
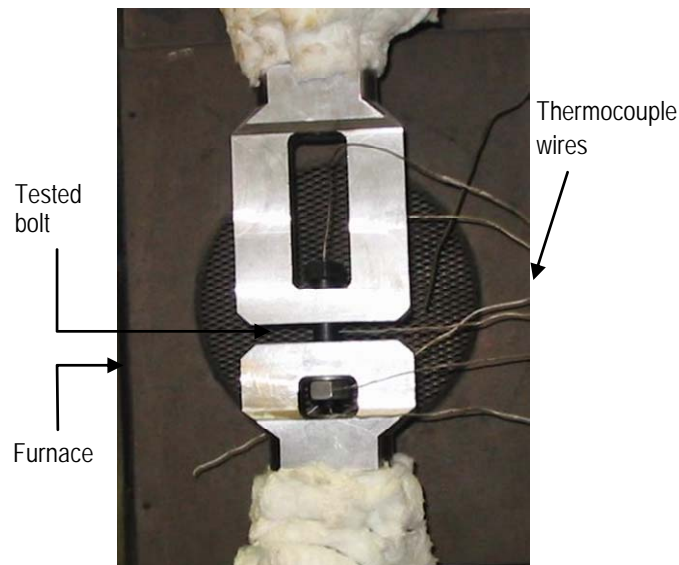

Figure 1: Test arrangement for structural bolts in tension (with permission of Hu et al. [16])

2.3 Test results at room temperature

The results of the room temperature tests on 8.8 high-strength structural bolts are shown in Fig. 2. The bolts are arranged in order of their number designations shown in Table 3. It can be found from the tests that structural bolts assembled with Property Class 10 nuts mostly failed by necking of the threaded portion of the bolt shank, while those with Property Class 8 nuts by thread stripping.

It should be noted that the failure mechanism might have been influenced by the coating process of nut threads. The Class 8 nuts were coated with a zinc layer, while the Class 10 nuts had a black oxidation coating to prevent corrosion [17]. The threads of nuts with zinc coating are believed to be over-tapped by a certain amount in thickness (about 0.4 mm [9]).

Johnson [18] recommended the clearance 6AZ6g for structural bolts and nuts with zinc coating plus an extra thickness reduction of 0.066 mm for placing a zinc layer in threads. According to BS 3643-1[19], ISO 10684[15] and ISO 965-5[10], the basic profiles for hot-dipped galvanized bolts and nuts may adopt 6AZ6g or 6AX6g as tolerance classes for internal and external threads. In addition to this, the British standard BS 4190 [11] indicates that when a thick protective coating is applied to a bolt of Grade 8.8 or 10.9, internal threads are required to be over-tapped to all for the extra coating thickness. The over-tapping process suggests that nut threads with zinc coatings may fail under the bolt tensile loading, as shown in the lower half of Fig. 2.

Table 3: Ultimate resistance of structural bolts at room temperature

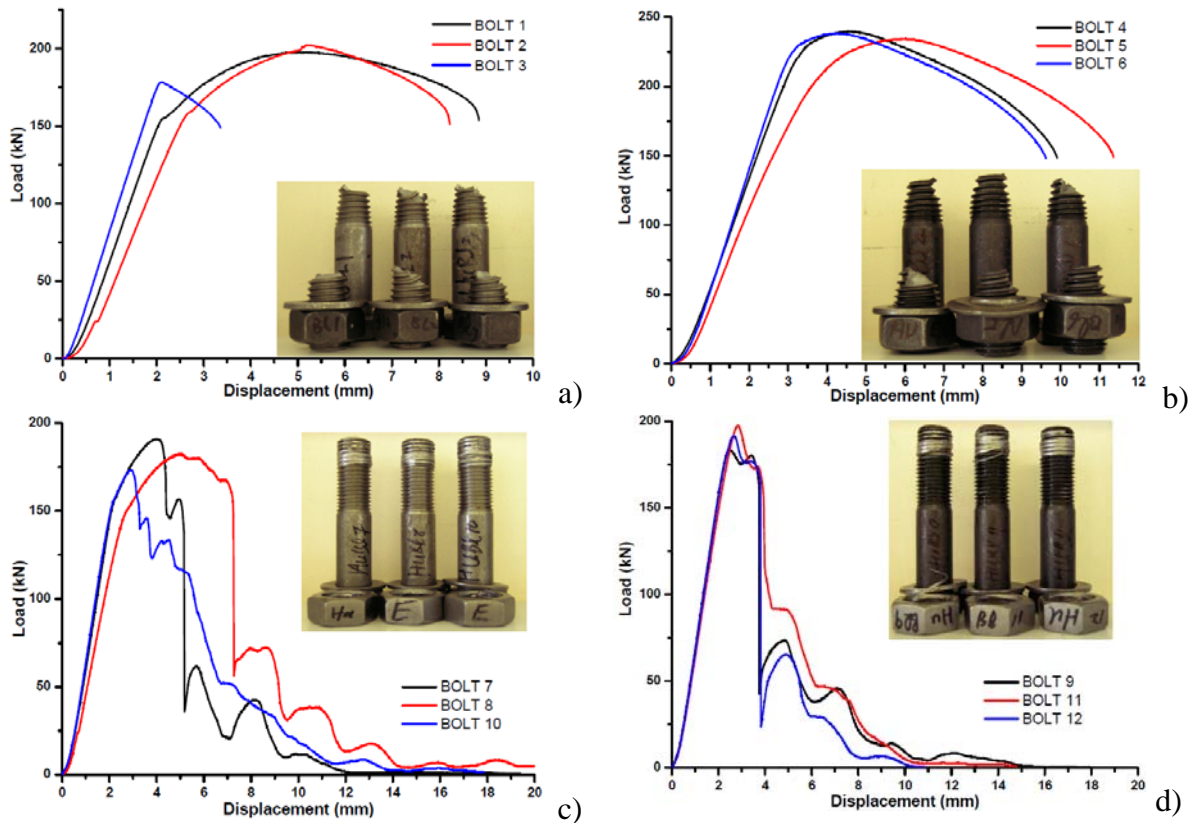| Bolt Sets	Bolt No.	Strength grade		Nut coating	Failure mode	Failure load (kN)	Tolerance class
		Bolt	Nut				
Bolt Group A	BOLT1 BOLT2 BOLT3	Grade 8.8	Property class 10	Black oxidation	Bolt breakage	197.8 202.3 178.5	7H/8g
Bolt Group B	BOLT4 BOLT5 BOLT6	Grade 8.8	Property class 10	Black oxidation	Bolt breakage	230.7 234.4 238.4	6H/6g
Bolt Group C	BOLT7 BOLT8 BOLT10	Grade 8.8	Property class 8	Zinc plating	Threads stripping	191.1 182.7 173.2	7H/8g
Bolt Group D	BOLT9 BOLT11 BOLT12	Grade 8.8	Property class 8	Zinc plating	Threads stripping	183.8 197.6 191.4	6H/6g

Figure 2: Performance of structural bolts at ambient temperatures: (a) Group A (b) Group B (c) Group C (d) Group D (with permission of Hu et al. [16])

2.4   Test results at high temperatures

A total of thirty-six bolts were tested under temperatures ranging from 20 ℃ to 600 ℃, and their failure loads are plotted in Fig. 3. All bolts collected in Table 4 failed by bolt breakage, with the only exceptions of BOLT18 and BOLT19 by thread stripping. It can be seen that there was a drastic reduction in the failure loads at high temperatures, which was consistent with the finding of Kirby [6]. Importantly, the

present experimental program found that using a nut one property class higher than the Grade 8.8 bolt did not always avoid failure by thread stripping, although it did so for most specimens as stated previously. The coating operation for components in groups A and B is black oxidation. A possible reason is the variation in the material properties and the temperature distribution among the components.

Table 4: Ultimate resistance of structural bolts at high temperatures

| Bolt Sets	Temp	Bolt No.	Failure load (kN)
Bolt Group A	150	BOLT13	197.7
		BOLT14	205.7
		BOLT15	200.1
	300	BOLT16	186.5
		BOLT17	178.1
		BOLT20	190.2
	400	BOLT31	140.0
		BOLT32	134.2
		BOLT33	133.1
	500	BOLT25	80.5
		BOLT26	75.9
		BOLT27	77.3
	600	BOLT37	38.5
		BOLT38	39.0
		BOLT39	39.1
Bolt Group B	150	BOLT18	229.8
		BOLT19	228.7
		BOLT21	232.9
	300	BOLT22	224.2
		BOLT23	218.1
		BOLT24	224.9
	400	BOLT34	189.8
		BOLT35	181.2
		BOLT36	178.4
	500	BOLT28	118.2
		BOLT29	108.3
		BOLT30	115.3
	600	BOLT41	49.7
		BOLT42	48.2
		BOLT43	48.9
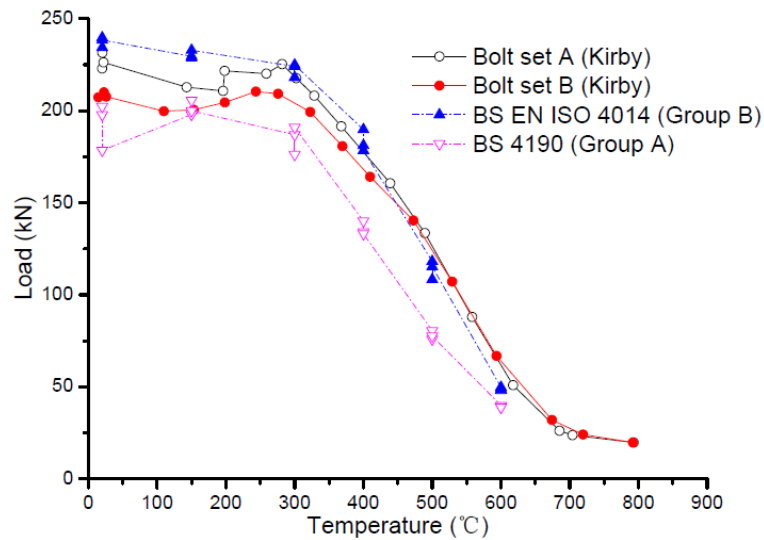
Figure 3: Failure loads at high temperatures

3   Finite element simulation

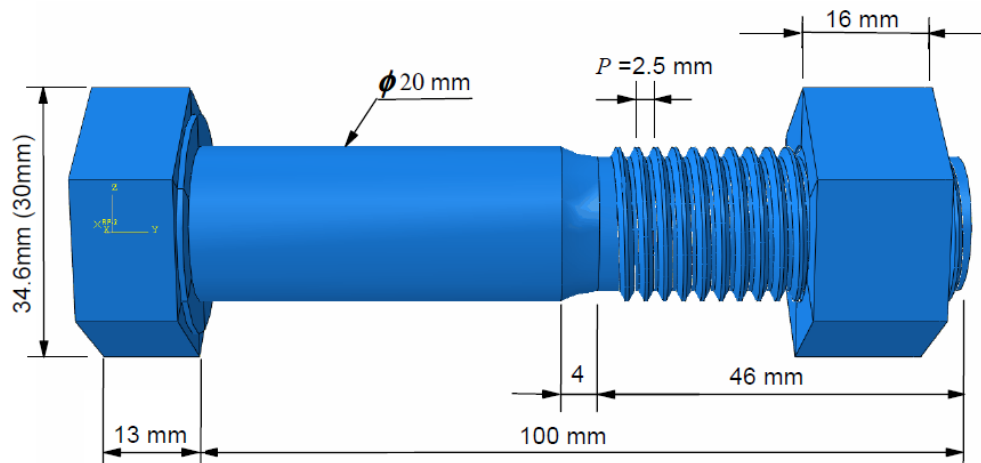### 3.1   Helical thread models for structural bolts

Figure 4: Geometrical details for a single fastener

In simulation of bolt performance in tension, the simplified approach was applying a two-dimensional FE model to represent a three-dimensional problem [20]. However, this simplification would result in stacking an appropriate number of threads in the threaded portion for the FE models, unable to catch helical effects in external and internal threads, e.g. loosening phenomena of bolted joints. Therefore, Fukuoka and Nomura [21] highlight that, when analyzing the mechanical behavior of bolted connections with three-dimensional analysis, it has been a common practice to use helical thread models for the threaded portion of bolts with asymmetrical geometry. The general details on geometrical dimension for a single fastener are illustrated in Fig. 4. In addition, as presented in the research work of Kirby [6] and Hu et al. [7], tolerance classes (the degree of fit) and over-tapping processes (for accommodating the extra zinc coating layer) may have an impact on bolt performance in tensile failure. Hence, internal and external threads have been set up for producing thread difference of tolerance classes in the numerical analysis. General details on tolerance classes for high strength hexagonal bolts are determined in accordance with specification of BS 4190 [11], BS 3692 [22] and BS EN ISO 4014 [23] for the

proposed helical thread model. Thread profile details are available in the specification of BS 3643-1 [19] and ISO 965-5 [10], as collected in Table 5.

Table 5: Dimension details of internal and external threads

Tolerance class		Internal threads				Tolerance class		External threads			
		Pitch	Major D	Pitch D2	Minor D1			Pitch	major d	pitch d2	minor d1
6H	Min	2.5	20.000	18.376	17.294	6g	Min	2.5	19.623	18.164	/
	Max	2.5	20.000	18.600	17.744		Max	2.5	19.958	18.334	16.891
7H	Min	2.5	20.000	18.376	17.294	8g	Min	2.5	19.428	18.069	/
	Max	2.5	20.000	18.656	17.854		Max	2.5	19.958	18.334	16.891
6AZ	Min	2.5	20.000	18.726	17.644	6az	Min	2.5	19.315	17.856	/
	Max	2.5	20.000	18.950	18.094		Max	2.5	19.650	18.026	16.583

In addition, these standards (BS 3643-1[19], ISO965-4 [24] and ISO 965-5 [10]) also present the specified tolerance classes for internal threads to mate with external threads without and with a heavy coating layer. In the standards, *tolerance class* is defined as a number and letter combination for indicating the degree of fit between internal and external threads, as shown in Fig. 5. The British standard [11] accepted the tolerance class 7H/8g as the specification, while the European standard [23] attempted to achieve a closer fit for bolt and nut threads, adopting 6H/6g in the standard. In addition, for protection of bolt threads, a thin, adherent uniform metallic layer (normally zinc-based) has been accounted for in the ISO standard through fundamental deviations, EI_{AX} or EI_{AZ} (tolerance position), for addressing a problem in reduction of thread size due to the over-tapping process, and the calculation method has been specified in the same ISO standard, with 6AX and 6AZ representing tolerance classes for internal threads. The thread profiles calculated for internal and external threads, comprising the maximum and minimum values for major, pitch and minor diameters, are available in Table 5 for their corresponding tolerance classes. In addition, the tolerance positions of threads are also demonstrated in Fig. 5, with 6H, 7H and 6AZ for nut threads and 6g, 8g and 6az for bolt threads.
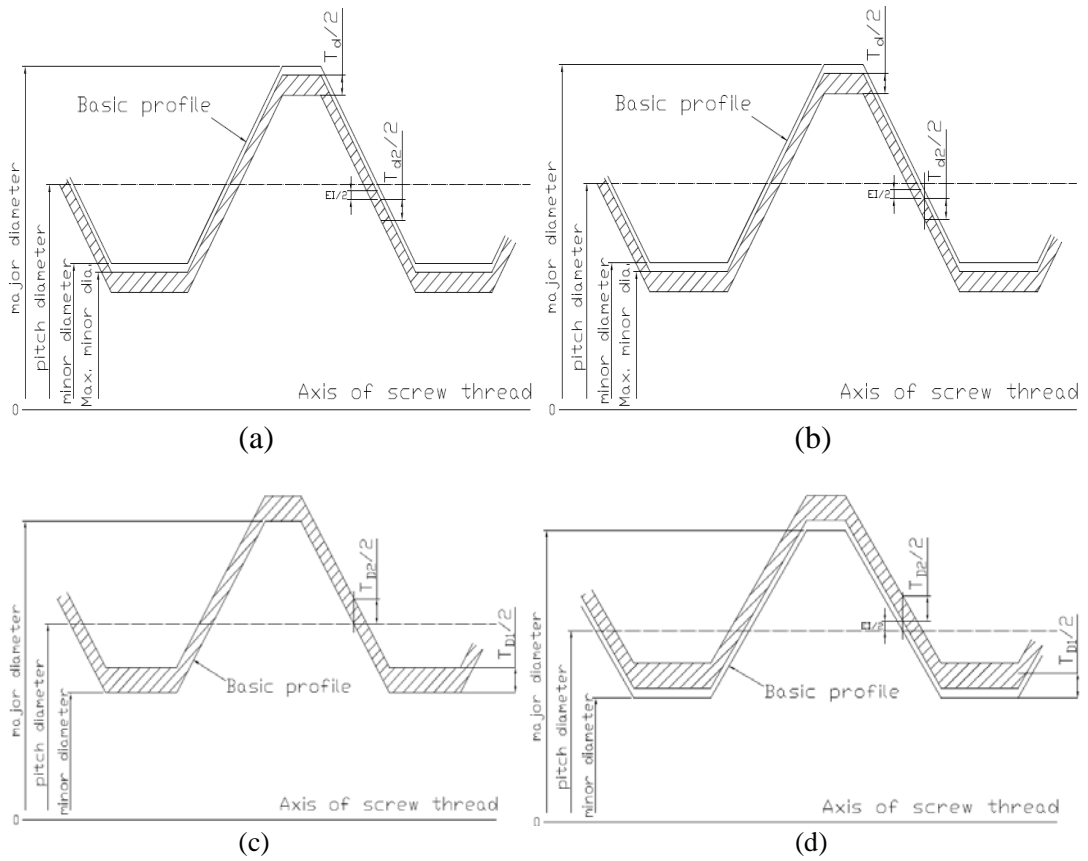
Figure 5: Thread profiles: a) tolerance position 6az for external threads; b) tolerance position 6g or 8g for external threads; c) tolerance position 6H or 7H for internal threads; d) tolerance position 6AZ for internal threads
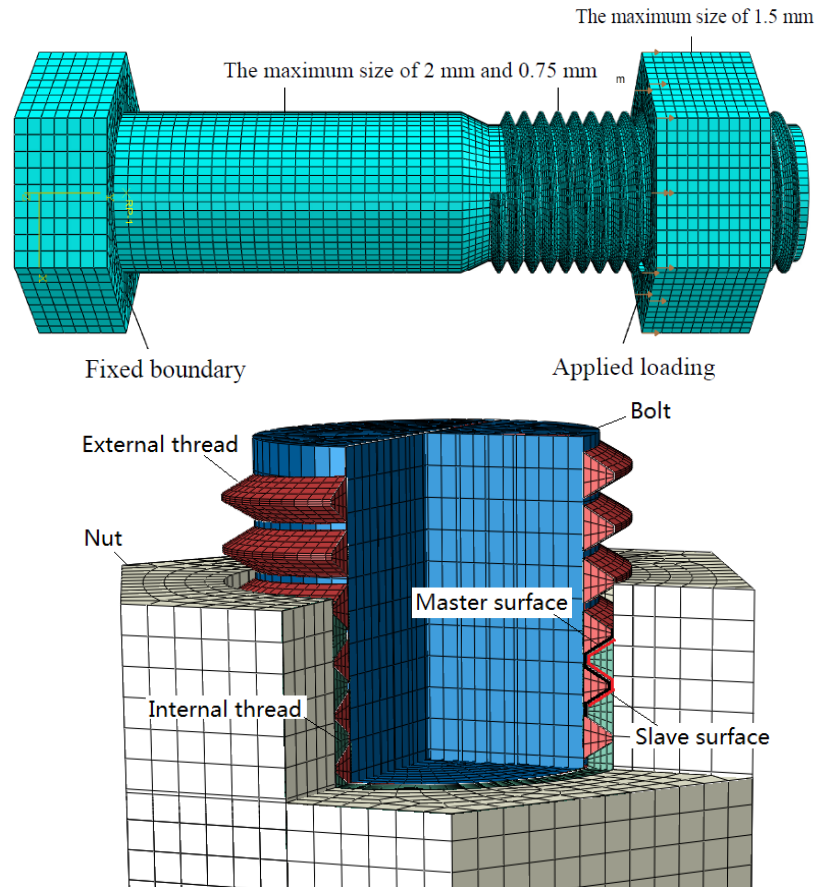
3.2   Models and boundary conditions

Figure 6: Finite element mesh with boundary conditions

Fukuoka and Nomura [21] advised researchers to use some sophisticated functions of commercial software for effective modeling. The mesh generation scheme proposed here may be executed with the help of commercial software e.g. Abaqus. The finite element mesh for a single bolt with its boundary conditions is illustrated in Fig. 6, applying 3D continuum hexahedral elements in the numerical analysis, recommended by Sherbourne and Bahaari [25]. Regarding the numerical model shown in Fig. 6, for the bolt cylinder, axial displacements are fully restrained at the bottom surface of a bolt, and the axial force is applied as a uniform displacement to a nut surface. For contact simulation, there are two formulations (small sliding and finite sliding) available for modeling the interaction between two contacting surfaces. Comparison has been performed for small sliding and finite sliding, and it has been realized that the small sliding formulation is less expensive in computation than the finite element sliding approach [26]. Regarding contact friction, Fukuoka and Nomura [21] state that coefficients of friction μ are varied from 0.05 to 0.20. Coefficient of friction 0.15 is employed within this study. Master surfaces and slave surfaces are specified for internal and external threads, as illustrated in Fig. 6. In addition, general details for integration methods, element types, contact formulations and applied displacements are collected in Table 6 for the simulation.

Table 6:   Detailed parameters of finite element model

Integration method	Element type	Contact simulation	Displacement applied
Bolt A Explicit	C3D8R	Small sliding	8mm
Bolt A Implicit	C3D8I	Small sliding	
Bolt C Explicit	C3D8R	Small sliding	4mm
Bolt C Implicit	C3D8I	Small sliding	

3.3   Numerical integration methods

Implicit and explicit resolutions have fully integrated eight-node isoparametric brick elements (C3D8I) and reduced integrated eight-node isoparametric elements (C3D8R) applied in simulation of bolt performance respectively. As illustrated in the figure, fully fixed constraints are applied to the hexagonal head of a single bolt, using the coupling function, and a very small speed is uniformly added onto the nut component in the numerical analysis. For the implicit dynamic procedure, integration operator matrices must be inverted and a set of nonlinear equilibrium equations must be solved at each time increment [26]. The explicit integration approach is based on the forward Euler method, which means that numerical displacements or velocities are calculated in terms of quantities known at the beginning of each time increment. As a consequence of this, the global mass and stiffness matrices need not be formed and inverted in the numerical analysis, which means that each time increment is relatively inexpensive compared to the increments in an implicit integration scheme [26]. These numerical models were run on a high performance computing workstation, containing 32 GB of RAM and two Intel Xeon E5 Hex-core CPUs.

3.3.1   Implicit model details

The implicit FEM method presents a solution through a tedious calculation procedure using Newton-Raphson iterations for enforcing equilibrium of internal forces with external loads applied on a structural model. Its computational cost is dependent on calculation of successive tangent matrices for fully integrated solid elements (C3D8I) applied in the numerical simulation. They are lower-order quadrilateral continuum elements enhanced with incompatible deformation modes, which is capable of modification of incorrect stresses and overestimated stiffness, eliminating artificial stiffening through adding internal degrees of freedom to the elements, and eventually resulting in improvement of the bending simulation [26]. The contact behavior has been simulated by using the finite sliding interaction approach, which enables researcher to define contact constraints between two surfaces (master surface generally assigned to the stiffer body with a coarser mesh), allowing for arbitrary translations and rotations between these interacting surfaces [27]. For a converged solution, small amounts of contact stabilization are recommended for the simulation. In addition, the initial increment of 0.2% has been taken into account in the numerical simulation with the maximum allowable increment size set at 10% (according to the manual).

3.3.2   Explicit model details

In the explicit analysis, computational cost relies on calculation of a large number of successive time increments for reduced integration elements (C3D8R) adopted in the simulation. Unlike the implicit procedure, this algorithm is dependent on the explicit central difference integration rule. Accelerations are calculated at the beginning of

the increment using the formula in Equation 1, where M^{NJ} is the mass matrix for the applied load vector $P^{J}_{(i)}$ and the internal force vector $I^{J}_{(i)}$.

$$\ddot{u}^{N}_{(i)} = (M^{NJ})^{-1}(P^{J}_{(i)} - I^{J}_{(i)}) \tag{1}$$

The explicit integration procedure requires a conditional stability limit for the central difference operator, which should be derived in terms of the highest frequency ω_{max} and the critical damping ξ_{max} in association with the aforementioned frequency in the system, as presented in Equation 2.

$$\Delta t \le \frac{2}{\omega_{max}}(\sqrt{1 + \xi^2_{max}} - \xi_{max}) \tag{2}$$

However, this stability limit may be approximated in terms of the material density ρ, the characteristic length of the smallest element L_e and the Lamé constants λ and μ, as formulated in Equation 3.

$$\Delta t \approx \min(L_e \cdot \sqrt{\frac{\rho}{(\lambda + 2\mu)}}) \tag{3}$$

As observed in this formula, the critical time increment is proportional to the size of the smallest elements and a very fine mesh may result in very small time increments, eventually increasing computation time. This time increment is also associated with the material density, which may be utilized for the mass scaling approach [28].

For the explicit integration procedure, the *general contact algorithm* has been in use for demonstrating the contacting interaction between internal and external threads in Fig. 6, which also adopted the finite-sliding formulation for nonlinear geometrical effects, including large deformations or large rotations. The frictional coefficient has been taken as 0.15 for contact pairs with a weaker enforcement of contact constraints through adopting the penalty contact algorithm, which is well suited for very general contact modeling.

As stated in the research paper of Adam et al. [28], the explicit analysis may need an incredibly large number of time increments for the numerical model, leading to very long computation time for simulation of quasi-static problems (normally requiring more than ten seconds). The Abaqus documentation recommends two numerical techniques for faster solutions: a) time scaling and b) mass scaling. Time scaling is determined as increasing deformation speed to apply displacements and/or loads in a shorter time period, provided that material characteristics are independent of the rate of deformation. However, the mass scaling technique is heavily based on the principle in Equation 3, artificially increasing the density of a numerical model to boost the minimum stable time increment. Nevertheless, higher densities might induce higher kinetic energy, if inappropriate values have been taken in the analysis. To approach a quasi-static solution more efficiently, a very small speed has been applied onto nuts using a fifth-order polynomial function [27]. The quasi-static solution may be deemed to be attained, as the ratio of the kinetic energy and internal energy is lower than 10% in the numerical model.

3.4 Material laws

It has been a common practice that structural bolts and nuts are made from low alloy or carbon steels, whose Young's modulus and Poisson's ratio are 200 GPa and 0.3,

respectively. Four different constitutive relationships, demonstrated in Fig. 7, can be used to represent engineering stress/strain curves for bolt materials, proposed in the research work of Hu et al. [29], Bahaari & Sherbourne [30] and Dessouki et al. [31]. The von Mises yield criterion is commonly applicable to the metal-based materials for prediction of the onset of yielding, and the behavior on further yielding is predicted by the associated 'flow rule' and hardening law. The bi-linear material model, shown in Fig. 7(a), assumes the onset of yielding at the strain ε_p corresponding to the proof stress, and simply uses the value of 5% as the ultimate strain for the bolt material. Bahaari and Sherbourne [30] presented a trilinear stress-strain model displayed in Fig. 7(b). The yield stress is considered to correspond to a proof strain of 0.006 and the ultimate strength is presumed at a strain of $8\varepsilon_p$. Dessouki et al. [31] modified the previous trilinear stress-strain relationship for the bolt material, as illustrated in Fig. 7(c), where the yielding strain is assumed as $3.0\varepsilon_p$, corresponding to the 'yielding' strength ($0.67f_u + 0.33f_{0.2p}$). The ultimate strength and strain adopted are the same as previously described. The final trilinear material model, as displayed in Fig. 7(d), assumes a yielding plateau between ε_p and $3\varepsilon_p$, and the ultimate strength is specified at a strain of 5% for the numerical analysis.
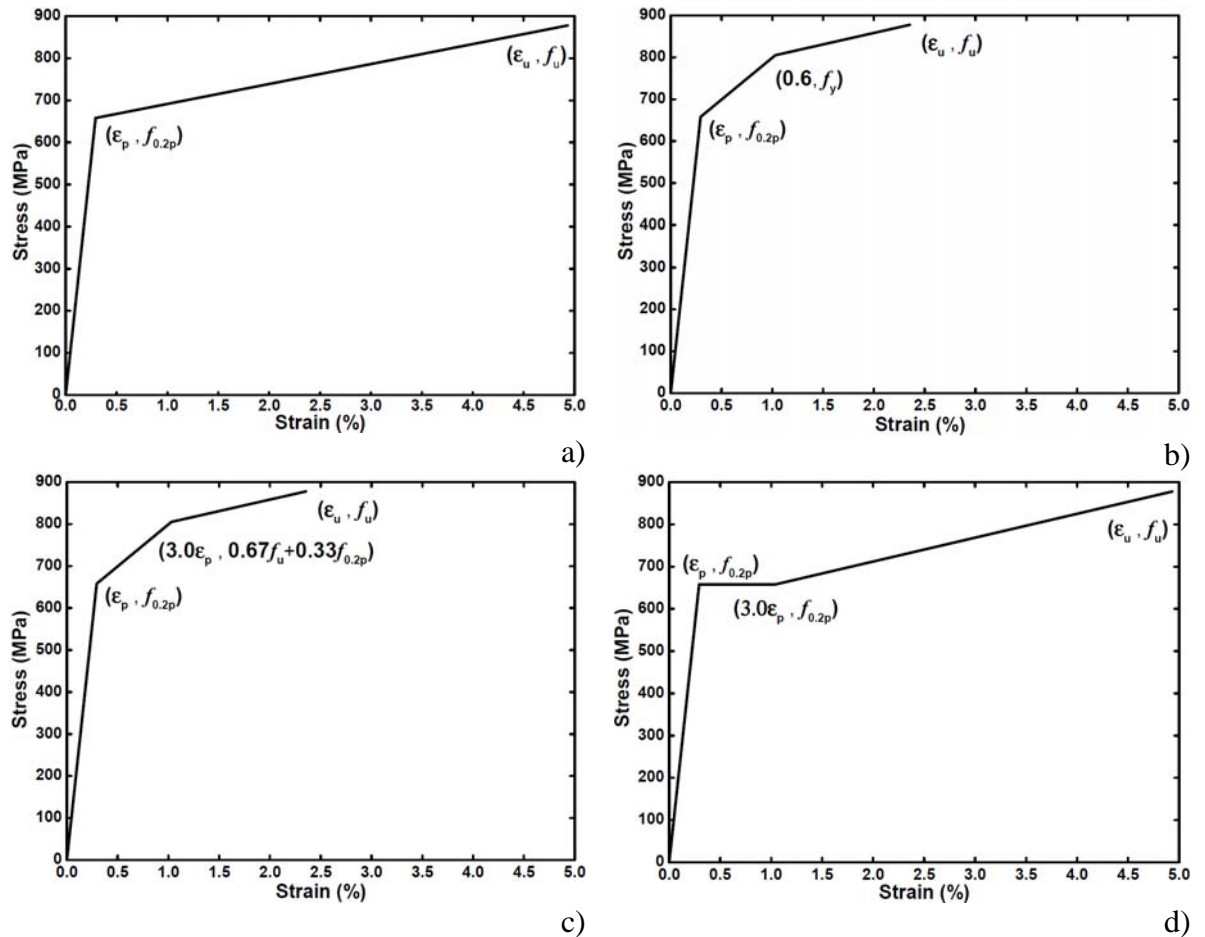

Figure 7: Material laws for bolt metals (a) Bi-linear model, (b) Trilinear model 1, (c) Trilinear model 2, (d) Trilinear model 3

4 Results and discussion

4.1 Sensitivity study

The Abaqus documentation states that it is safe to assume that performing an analysis in a natural time scale will produce accurate static results for analysis of a real-life event. However, a dynamic procedure should be able to capture this process as well through increasing the loading rate in the solution so that the same physical event can be analyzed in a shorter time scale as long as the solution remains nearly the same as the static solution with insignificant dynamic effects. For analysis of bolt performance in tension, a sensitivity study has been carefully performed on the loading rates applied in both explicit and implicit integration procedures, which covers the loading values of 0.25 mm/s, 1mm/s and 5mm/s, indicated in Table 7, for the numerical simulations. If the numerical integration procedure is quasi-static, work done by external forces is nearly equal to internal energy stored in a physical system. For simulation to achieve the static performance, the ratio of kinetic energy to internal energy was recorded throughout the simulation, plotted in Fig. 8(a). As a generally accepted rule, the kinetic energy of the deforming material should not be observable throughout most of the simulation, not exceeding a small fraction (5% to 10%) of the internal energy, in which case the numerical procedure may be regarded as a quasi-static analysis. As illustrated in Fig. 8, three different loading rates have been examined for identification of the applicable value for the analysis, and the load displacement curves are also plotted corresponding to each loading value. It has been observed in this figure that the value of 0.25 mm/s produces more reliable numerical results in analysis of bolt performance. The static analysis may be presumed in this case, as the kinetic energy after 0.5 s is smaller than 5% of the total internal energy. In addition, the load-displacement relationships illustrated in Fig. 8(b) demonstrate that a crimped curve for the loading rate of 5 mm/s produced observable dynamic effects in the analysis. In view of these arguments, the lower loading rates (1mm/s or 0.25 mm/s) may be recommended for the analysis following the sensitivity study.

In addition to studying the loading rates, the ratio of kinetic energy to internal energy has been derived from numerical simulations for different constitutive models and numerical procedures, as illustrated in Fig. 9, which has been carefully examined throughout the loading process for achieving a reliable numerical procedure. In these plots, the energy of the deforming material observed from dynamic effects is not in excess of 5% to 10% of its internal energy throughout most of the numerical process. Therefore, the quasi-static analysis may be presumed after this sensitive study, following the statements in the preceding discussion.

When loading a bolt component, the initial stage, within 0-1s, is definitely a dynamic procedure. The dynamic response is therefore observed for the numerical simulation, with a sudden increase in energy ratio. Another point for the dynamic response is the component failure procedures, which is normally at the end of the numerical procedures. The near vertical lines in Figs. 8(a), 8(c) and 9, at the starts and ends of some simulation runs, demonstrate these effects.
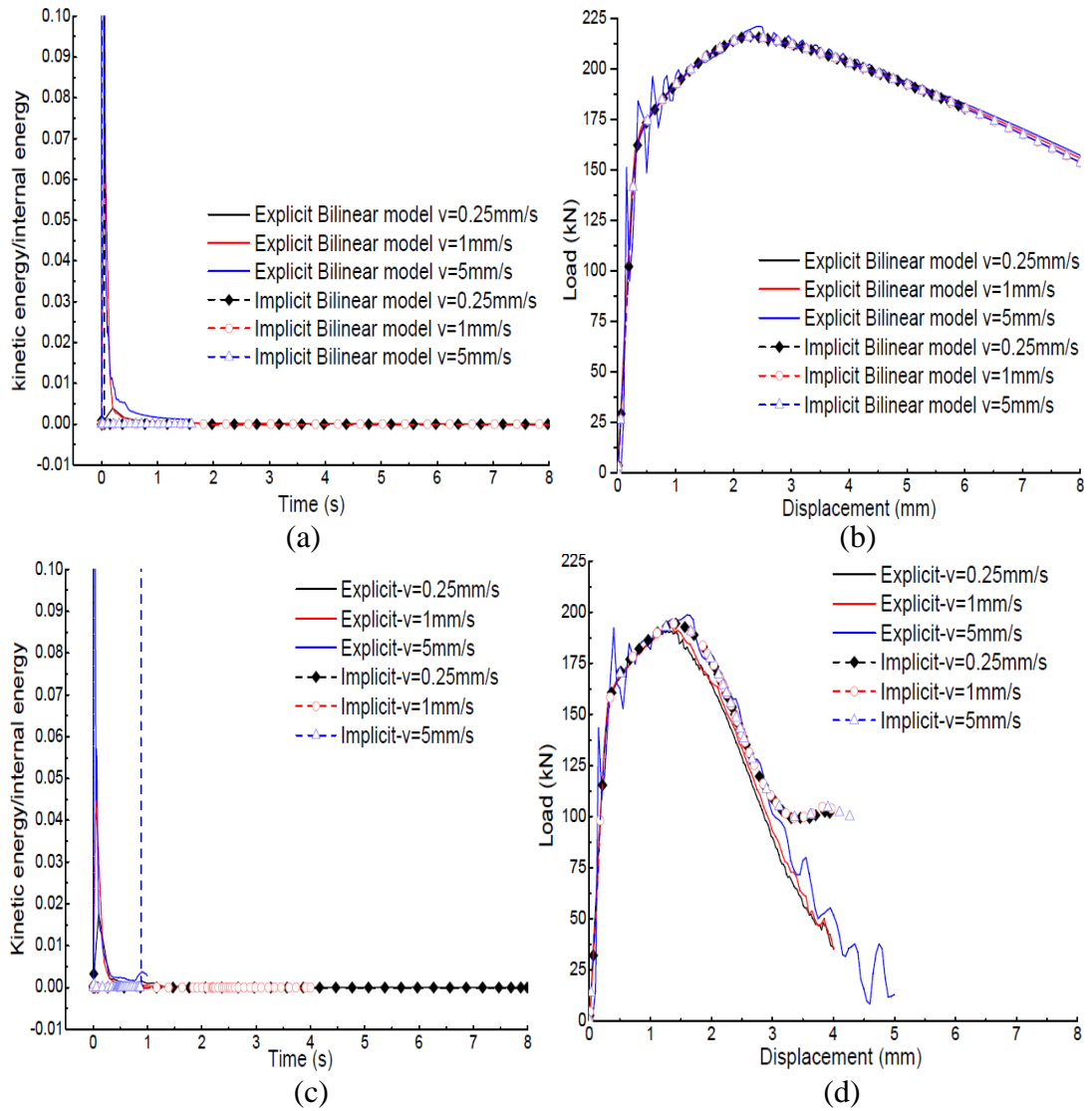
Figure 8: Sensitivity study: (a) energy comparison in Group A, (b) load-displacement curves in Group A, (c) energy comparison for Group C, (d) load-displacement curves for Group C
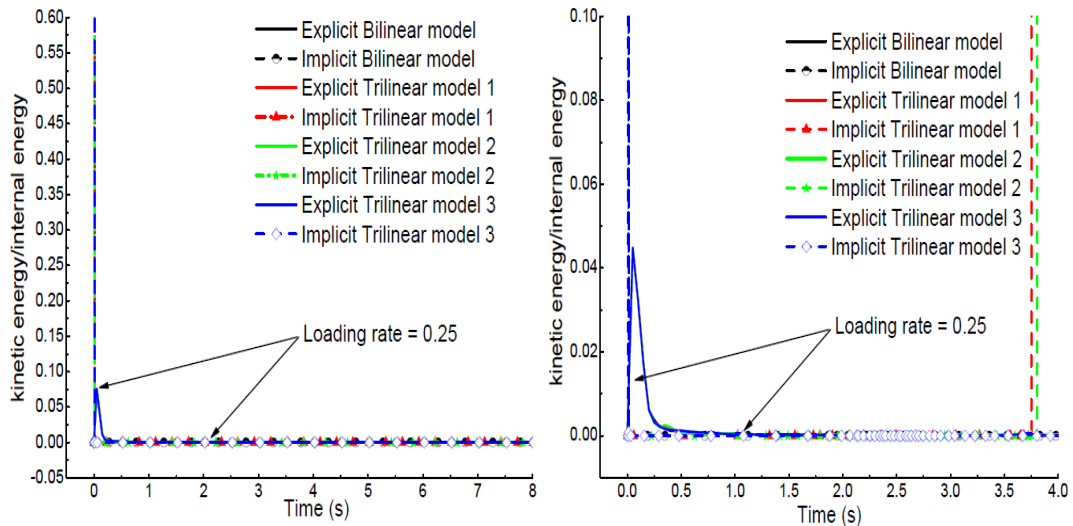
Figure 9: Ratio of kinetic energy to internal energy: (a) bolts in Group A; (b) bolts in Group C (Loading rate = 0.25 mm/s)

Table 7:   Results of parametric analysis

	Applied velocity (mm/s)	Displacement at the maximum load (mm)	Maximum load (kN)
Bolt A Explicit	0.25	2.31	216.1
	1.00	2.25	216.1
	5.00	2.45	220.9
Bolt A Implicit	0.25	2.29	216.0
	1.00	2.26	216.0
	5.00	2.26	216.0
Bolt C Explicit	0.25	1.28	191.10
	1.00	1.35	192.85
	5.00	1.60	198.74
Bolt C Implicit	0.25	1.41	194.45
	1.00	1.40	194.50
	5.00	1.39	194.49

4.2   Failure mechanisms and ultimate capacities

Failure of structural bolts in the simulation has been plotted in Fig. 10, compared with bolt failure mechanisms in experimental testing. It is obvious that a consistency has been achieved in their failure mechanisms for structural bolts between numerical analysis and experimental testing, identified as necking of the threaded portion of the bolt shank for Group A and threads stripping for Group C. However, the numerical analysis is unable to declare the fracture mechanism for these components. Also, no failure criteria have been introduced into the numerical simulation.
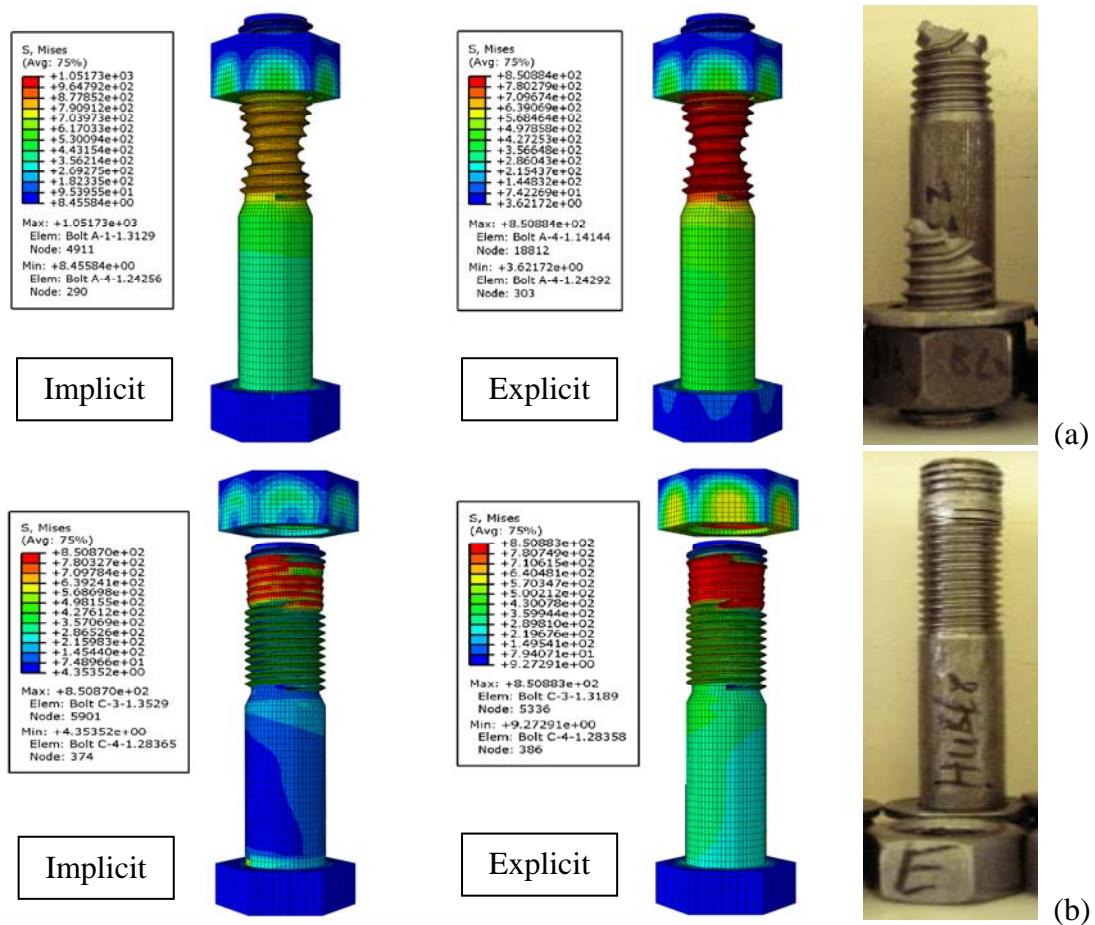
Figure 10: Failure mechanisms: (a) bolt shank failure in Group A; (b) threads stripping in Group C

This study applied implicit and explicit time integration procedures for analysis of tensile performance of structural bolts using four different constitutive relationships. The numerical results, collected in Table 8, generally indicate that the ultimate capacities produced for bolts in Group A (average 200.1 kN) are relatively higher than the ones in Group C bolts (average 182.3 kN), which clarifies the impact of different failure mechanisms on the bolt capacities, caused by tolerance classes in bolt threads. In addition, the numerical prediction has been compared with the test average recorded in experiments. The numerical analysis slightly overestimates the ultimate capacities of high-strength bolts in practice. In addition, the numerical prediction has also been compared with the nominal value of 196kN, stipulated in European standard BS EN ISO 898-1 [32]. The nominal value from the standard is slightly higher than the prediction in numerical procedures for the bolts with the failure of threads stripping, and lower than the load capacities of bolts with the bolt shank failure from the numerical analysis.

Table 8: Ultimate capacities of structural bolts

Group classification	Constitutive relationship	Numerical results (kN)	Error (%)
Bolt A Explicit	Bilinear model	220.9	10.39
	Trilinear model 1	219.4	9.65
	Trilinear model 2	217.4	8.65
	Trilinear model 3	216.2	8.05
Bolt A Implicit	Bilinear model	216.0	7.95
	Trilinear model 1	219.3	9.60
	Trilinear model 2	217.3	8.60
	Trilinear model 3	215.7	7.80
Bolt C Explicit	Bilinear model	192.8	5.76
	Trilinear model 1	199.0	9.16
	Trilinear model 2	197.5	8.34
	Trilinear model 3	189.6	4.00
Bolt C Implicit	Bilinear model	194.5	6.69
	Trilinear model 1	197.9	8.56
	Trilinear model 2	196.7	7.90
	Trilinear model 3	191.5	5.05

4.3 Load-displacement curves

For investigation of behavior of structural bolts, force-displacement relationships are taken into account as an evaluation index. Hanus et al. [12] highlighted two aspects which may affect the force-displacement curves. First, these force-displacement curves are not linear for low load levels, due to extra displacements induced from connection clearance, whereas the behavior of the steel material might still be elastic. Second, the test rig may deform in the experimental testing, and its elongation may contribute to the displacements taken from the referential points on the loading jacks in the machine [12]. Furthermore, an analytical approach has been recommended for reducing the 'noises' caused by the test rig deforming, and connection clearance may be removed through the pre-loading procedure. In this method, the test rig deformation may be regarded as in the elastic region during the complete testing. The elastic elongation of a bolt may be calculated based on Eurocode values allowing for a determination of the elastic stiffness of the test rig. As a consequence, the elastic deformation of the test rig can be taken away from the force-displacement curves, as illustrated in Fig. 11.
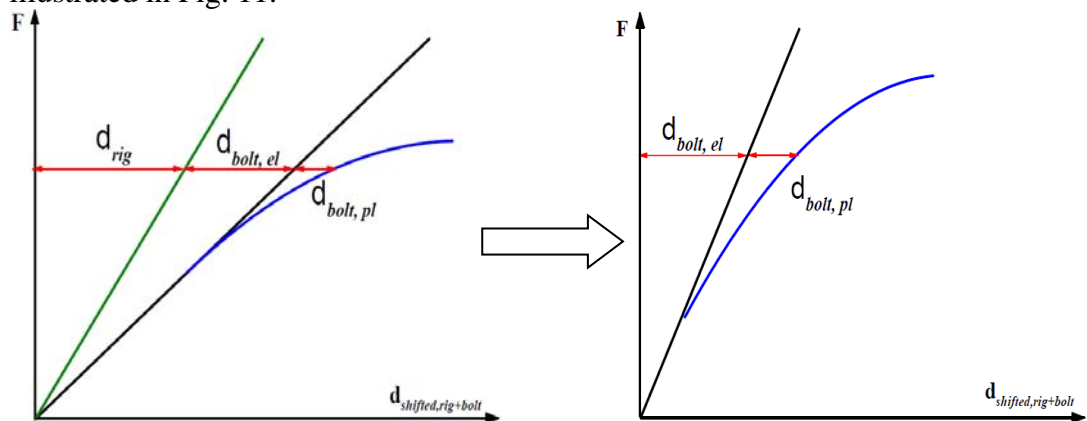

Figure 11: Elimination of parasitic deformation from the test rig (with permission of Hanus et al. [12])

In experimental results of Hu et al. [16], the force-displacement curves also included these deformations, which needs to be removed for deriving the corresponding force-displacement curves for Grade 8.8 structural bolts. The preceding method has been adopted to modify the force-displacement curves recorded from experimental tests, intended to remove the contribution of testing device deforming in these curves.

After numerous simulations, a comparative analysis was executed for different force-displacement relationships, with consideration of the constitutive material models already illustrated. Previously the simulation represented two failure mechanisms of structural bolts, and then their load bearing capacities were retrieved at the maximum limit. The force-displacement curves derived from both experiments and numerical simulations are illustrated in Fig. 12. From these results, it must be very obvious that different failure mechanisms may be a primary reason in producing different limiting load capacities of structural bolts. After removing the deformation of testing device, the modified force-displacement curves received are in very good agreement with numerical outputs recorded. Apart from this, the analytical procedure proposed by Hanus et al. [12] has been proved to be effective in practice on processing the valuable test data.
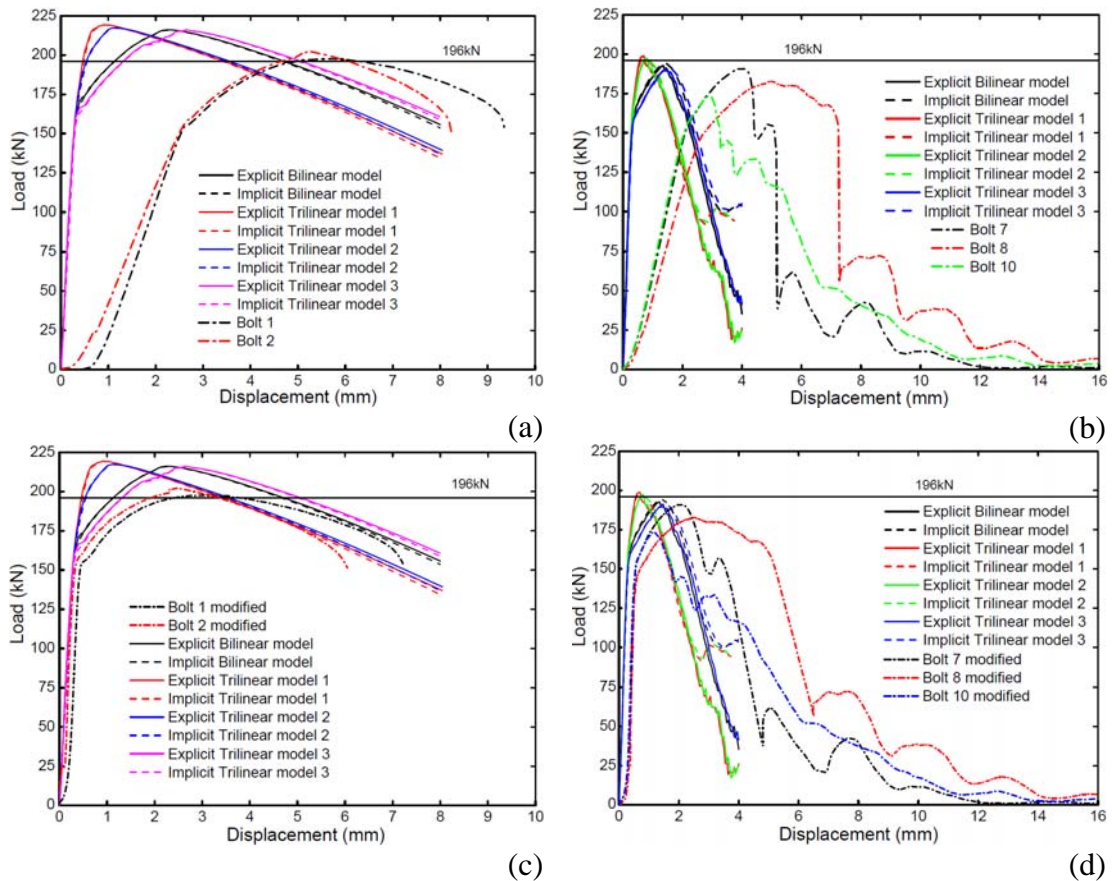

Figure 12: Study of force-displacement curves for different material models

Previous discussion tends to be focused on comparison of force-displacement curves in numerical simulations and experimental data, adopting one material law. Nevertheless, influence of various constitutive models on bolt performance may be worthy of further investigation. As a consequence, the force-displacement curves

produced from the numerical simulations considered different constitutive material laws, as illustrated in Fig. 7. In accordance with the European standard (BS EN ISO 4014/4017), the yielding and ultimate loads (161 kN and 196 kN) are derived analytically for structural bolts, displayed in Fig. 13. Then the numerical analysis has been performed through implicit and explicit integration procedures. From these numerical simulations, it can be seen that before the yielding limit (161 kN), forces and displacements recorded are almost identical for all the plotted curves in Fig. 13. After the material yielding, the load-deformation relationships for Bilinear model and Trilinear model 3 are almost consistent in the numerical analysis. In a similar way, the plotted curves for Trilinear model 1 and Trilinear model 2 are in good agreement with each other in the displayed figure below. In addition to this, the numerical simulation discovered that the bearing capacity of a single bolt was highly dependent on its failure mechanism. The numerical models with bolt shank failure gave higher bearing capacities in comparison with the nominal value calculated from the standards. For bolts failed with threads stripping, the numerical models might underestimate the peak values in the analysis.
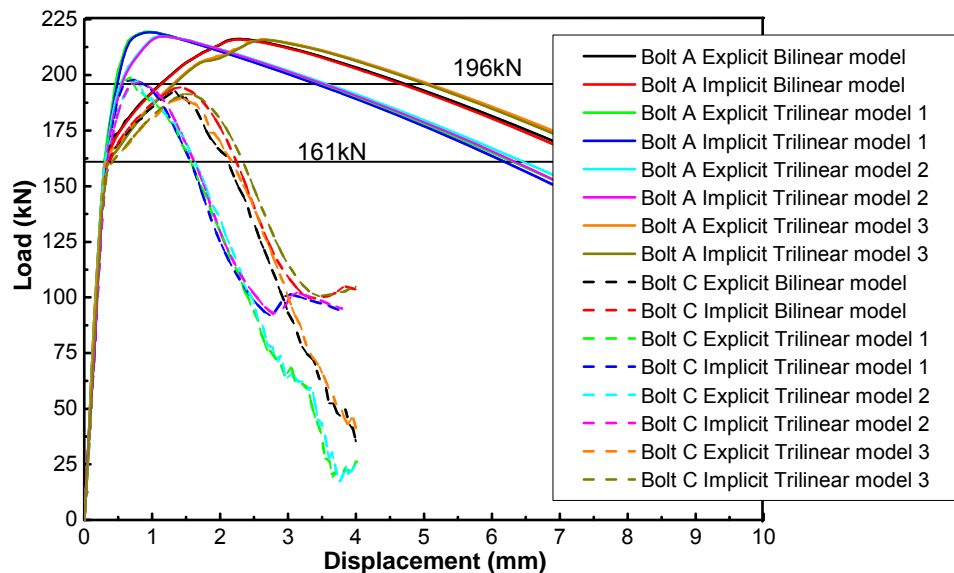

Figure 13: Numerical results for different constitutive laws

5 Concluding remarks

In this study, research efforts were primarily focused on verifying an assumption, suggested by BS 4190 [11] and Kirby [6], to prevent the premature failure of 8.8 structural bolts under normal and fire conditions. Failure of these components was observed for different tolerance classes from the coating operation after the experimental program. A number of findings can be summarized as follows:

- Most 8.8 structural bolts mating with nuts of one property class higher can lead to a higher probability in failure with ductile necking of the threaded portion of the bolt shank
- 8.8 structural bolts mating with bright nuts failed by thread stripping, due to threads of nuts was over-tapped for the coating process

- In the numerical simulation, different material models were taken into account for assessment of the mechanical performance of structural bolts under tensile loading. Influence of different material laws was small although some discrepancy in load-displacement relationship can be observed.
- The numerical simulation was capable of representing the failure mechanisms of 8.8 high-strength structural bolts, confirming that failure of thread stripping was due to different tolerance classes introduced for the coating process.

ACKNOWLEDGEMENTS

REFERENCES

[1] D.A. Nethercot, T.Q. Ahmed, B. Li, Unified classification system for beam-to-column connections, Journal of Constructural Steel Research, 45 (1) (1998) 39-65.

[2] Y. Goto, S. Miyashita, Validity of classification systems of semi-rigid connections, Engineering Structures, 17 (8) (1995) 544-553.

[3] U. Kuhlmann, A. Furch, Rotation capacity of steel joints, in: COST-C1 working group meeting, Helsinki, Finland, 1997.

[4] Y.C. Wang, J.B. Davison, I.W. Burgess, H.X. Yu, R.J. Plank, C.G. Bailey, The safety of common steel beam/column connections in fire, The Structural Engineer, 88 (21) (2010) 26-35.

[5] M.H.R. Godley, F.H. Needham, Comparative tests on 8.8 and HSFG bolts in tension and shear, The Structural Engineer, 60 (3) (1983) 21-26.

[6] B.R. Kirby, The behaviour of high-strength grade 8.8 bolts in fire, Jouarnal Constructural Steel Research, 33 (1-2) (1995) 3-38.

[7] Y. Hu, J.B. Davison, I.W. Burgess, R.J. Plank, Fire perfromance of grade 8.8 structural bolts, in: Eurosteel 2011, Budapest, Hungary, 2011.

[8] J. Laurilliard, Fastener coatings, in: J.H. Bickford, S. Nassar (Eds.) Handbook of Bolts and Bolted Joints, Marcel Dekker, New York, 1998, pp. 75-106.

[9] W. Wallace, Bolt Coating Thickness & Nut Overtapping - A Lesson in Practical Necessity, @ www.appliedbolting.com/pdf/Coated_Bolts_and_Overtapping.pdf, 2015.

[10] ISO, ISO 965 general purpose metric screw threads - Tolerances - Part 5: Limits of sizes for internal screw threads to mate with hot-dip galvanized external screw threads with maximum size of tolerance position h before galvanizing, International Organization for Standardization, Switzerland, 1998.

[11] BSI, BS 4190: ISO metric black hexagon bolts, screws and nuts - Specification, British Standards Institution, London, 2001.

[12] F. Hanus, G. Zilli, J.-M. Franssen, Behaviour of Grade 8.8 bolts under natural fire conditions-Tests and model, Journal of Constructural Steel Research, 67 (2011) 1292-1298.

[13] G.B. Lou, R. Wang, S. Yu, G.Q. Li, Mechanical properties of high-strength bolts after fire, Proceedings of the Institution of Civil Engineers-Structures and Buildings, 165 (SB7) (2012) 373-383.

[14] G.W. Owens, B.D. Cheal, Structural Steelwork Connections, Butterworths, London, 1989.

[15] ISO, ISO 10684: Fasteners - hot dip galvanized coatings,International Organization for Standardization, Switzerland, 2004.

[16] Y. Hu, J.B. Davison, I.W. Burgess, R.J. Plank, Comparative study of the behavior of BS 4190 and BS EN ISO 4014 bolts in Fire, in: Y.C. Wang (Ed.) 3rd international conference on steel and composite structures, Manchester, UK, 2007.

[17] R.T. Barrett, Fastener Design Manual, Natinal Aeronautics and Space Administration, Ohio, 1990.

[18] L. Johnson, Microstructural Characterisation of Structural Bolt Assemblies in Fire, PhD thesis, The University of Sheffield, Sheffield, 2014.

[19] BSI, BS 3643-1: Specification for ISO metric screw threads - Part 1: Principles and basic data, British Standards Institution, London, 1981.

[20] J.J. Chen, Y.S. Shih, A study of the helical effect on the thread connection by three dimensional finite element analysis Nuclear Engineering and Design, 191 (1999) 109-116.

[21] T. Fukuoka, M. Nomura, Proposition of helical thread modelling with accurate geometry and finite element analysis, Journal of Pressure Vessel Technology, 130 (2008) 0112041-0112046.

[22] BSI, BS 3692: ISO metric precision hexagon bolts, screws and nuts - Specification, British Standards Institution, London, 2001.

[23] CEN, BS EN ISO 4014: Hexagon head bolts - Products grades A and B, European Committee for Standardisation, Brussels, 2001.

[24] ISO, ISO 965 general purpose metric screw threads - Tolerances - Part 4: Limits of sizes for hot-dip galvanized external screw threads to mate with internal screw threads tapped with tolerance position H or G after galvanizing, International Organization for Standardization, Switzerland, 1998.

[25] M.R. Bahaari, A.N. Sherbourne, Finite element prediction of end plate bolted connection behavior II: analytical formulation, Journal of Structural Engineering, ASCE, 123 (1997) 165-175.

[26] ABAQUS, Standard user's manual, Hibbitt, Karsson and Sorensen, Inc, 2014.

[27] B. Egan, C.T. McCarthy, M.A. McCarthy, P.J. Gray, R.M. Frizzell, Modelling a single-bolt countersunk composite joint using implicit and explicit finite element analysis, Computational Materials Science, 64 (2012) 203-208.

[28] C. Adam, S. Bouabdallah, M. Zarroug, H. Maitournam, Stable time step estimates for NURBS-based explicit dynamics, Computer Methods in Applied Mechanics, 295 (2015) 581-605.

[29] Y. Hu, J.B. Davison, I.W. Burgess, R.J. Plank, Multi-Scale Modelling of Flexible End Plate Connections under Fire Conditions, The Open Construction and Building Technology Journal, 4 (2010) 88-104.

[30] M.R. Bahaari, A.N. Sherbourne, 3D simulation of bolted connections to unstiffened columns - II. Extended endplate connections, Journal of Constructural Steel Research, 40 (3) (1996) 189-223.

[31] A.K. Dessouki, A.H. Youssef, M.M. Ibrahim, Behavior of I-beam bolted extended end-plate moment connections, Ain Shams Engineering Journal, 4 (4) (2013) 685-669.

[32] CEN, BS EN ISO 898-1: Mechanical properties of fasteners made of carbon steel and alloy steel - Part 1: Bolts, screws and studs, European Committee for Standardisation, Brussels, 2001.